Resolving the Rise and Fall of Star Formation in Galaxies
Proceedings IAU Symposium No. 373, 2023
T. Wong & W.-T. Kim, eds.
doi:10.1017/S1743921322004410

What Drives Galaxies from the Main Sequence to the Green Valley?

Lihwai Lin

Institute of Astronomy & Astrophysics, Academia Sinica, Taipei 10617, Taiwan

Abstract. Green valley galaxies (by selection) exhibit lower specific star formation rates and are thought to be in the transition from the active star-forming phase to the quiescent state. Physical mechanisms responsible for the depleted star formation in green valley galaxies, however, are still under debate. Using the ALMA-MaNGA Quenching and STar formation (ALMaQUEST) CO observations, we study the so-called 'resolved star formation scaling relations', which describe relationships among surface densities of star formation rate, stellar mass, and molecular gas mass. By comparing the kpc-scale scaling relations between the main sequence and green valley galaxies, we are able to quantify if the deficit of star formation in green valley galaxies is driven by depleted molecular gas or inefficient star formation. And finally, we present our recent ALMA dense gas (HCN and HCO^+) observations for a set of selected ALMaQUEST galaxies to discuss whether the green valley galaxies lack dense molecular gas or not.

Keywords. Galaxies; Molecular Gas; Galaxy Evolution

1. Introduction

The distributions of galaxies on the star formation rate (SFR) and the stellar mass (M_*) plane have been widely used to constrain the galaxy evolution models. In particular, the star-forming galaxies show a tight relation between the global SFR and M_*, referred to as the 'star-forming main sequence', across a wide range of redshifts (SFMS or MS; Noeske et al. 2007; Daddi et al. 2007; Lin et al. 2012; Whitaker et al. 2012; Speagle et al. 2014). Not only we want to know why there exists the star-forming main sequence, but also we want to understand under what kind of condition galaxies depart from the main sequence and become quiescent. To address theses questions, we focus on two issues, the molecular gas and the spatially resolved properties.

First, we need to bring the molecular gas into the whole picture because it is the direct fuel of star formation. Among the three variables, SFR, M_*, and molecular gas mass (M_{H_2}), we know that the relation between SFR and M_{H_2} has already been intensively studied, namely the Schmidt-Kennicutt Relation (SK relation; Schmidt 1959; Kennicutt 1998). This can be easily understood because the star formation is closely linked to how much gas is available. Compared to the SK relation, the origin of the relation between SFR and M_*, is less clear. In particular, M_* is simply the SFR integrated over time, and it is not physically intuitive why the current star formation has a strong dependence on its past history. On the other hand, the 3rd scaling relation between M_* and M_{H_2}, although not highlighted as intensively as the other two scaling relations, can be qualitatively understood as the consequence of the fact that both the gas and stellar components trace the underlying gravitational potential. Studying the gas content of galaxies is therefore essential if we want to gain a full picture about the link between star formation and M_*.

In addition to the gas, it has been recently acknowledged that the spatially-resolved observations offer a promising prospect to understand the quenching process. This is

because different quenching mechanisms will lead to different patterns in the spatial distributions of gas and SF (e.g. Lin et al. 2017). For example, in the case of ram-pressure stripping, the quenching can be outside-in, and in the case of AGN, the quenching is likely to proceed from the inner part to the outer part of galaxies. Therefore, the combination of spatially-resolved observations in both gas and stars gives clues about the nature of the quenching mechanisms.

The ALMaQUEST survey (Lin et al. 2020), standing for the ALMA-MaNGA quenching and star formation, is designed to offer spatially resolved molecular gas observations that have matched spatial resolutions to the MaNGA galaxies. In total, we observe 46 MaNGA-selected galaxies in CO(1-0) at kpc scales. We target three classes of galaxies, from starburst, the main sequence, to the green valley galaxies, allowing us to probe the gas content across different populations. In addition to ALMaQUEST, there are other surveys that also offer statistical samples with spatially resolved observations, for example, the EDGE-CALIFA (Bolatto et al. 2017), COMING (Sorai et al. 2019), and PHANGS-ALMA (Leroy et al. 2021) surveys, etc., enabling detailed studies of the interplay between gas and stellar populations at kpc or subkpc scales. Compared to ALMaQUEST, the sample sizes of EDGE-CALIFA and COMING are two or even three times bigger, and the spatial resolution of PHANGS is almost 10 times better. However, the main strength of ALMaQUEST is that it samples a wider range in terms of sSFR of galaxies and galaxy properties. In addition to the main sample that covers from SB to GV mentioned here, we are now continuing to add other classes of samples like AGNs and mergers.

2. Star Formation Scaling Relation for Main Sequence Galaxies

Using the spatially resolved measurements, there have been many studies quantifying the scaling relations among the SFR, M_*, and M_{H_2} surface densities on local scales (e.g. Lin et al. 2019; Brownson et al. 2020; Morselli et al. 2020; Sánchez et al. 2021; Ellison et al. 2021; Pessa et al. 2021). For star-forming regions in MS galaxies, these three parameters are strongly correlated with each other in the 3-D space as shown in Fig. 1, and each pair forms a tight sequence, corresponding to the resolved star-forming main sequence (rSFMS), resolved Schmidt-Kennicutt (rSK) relation, and resolved molecular gas main sequence (rMGMS; Lin et al. 2019), respectively. In Lin et al. (2019) we have performed a variety of analyses, which demonstrate that the rSFMS is likely a consequence of the other two relations that are more physically motivated. For example, the correlation coefficient is weaker for rSFMS than for the other two relations. We have also performed the partial correlation, showing that the SFR is primarily driven by M_{H_2}, and once that is taken into account, there is no additional dependence on the stellar mass. Nevertheless, the interpretation of this is still under debate, and there are also other hypotheses proposed by other people Sánchez et al. (see 2021, for an alternative explanation).

3. Star Formation Scaling Relation for Green Valley Galaxies

The above relations are obtained based on well-selected star-forming spaxels of main-sequence galaxies. Then what about galaxies departing from the MS, for instance, the green valley (GV) galaxies? One thing worth paying attention to is that GVs consist of not only star-forming spaxels but also a significant fraction of non-star-forming spaxels, for example, the retired spaxels. Therefore, in addition to separating the MS and GV galaxies, in Lin et al. (2022) we also separate the star-forming and retired spaxels using their locations in the BPT diagram. The retired spaxels are defined as those with Hα equivalent width (EW) less than 3 angstroms. These are the regions that we believe are no longer with active star formation.

https://doi.org/10.1017/S1743921322004410 Published online by Cambridge University Press

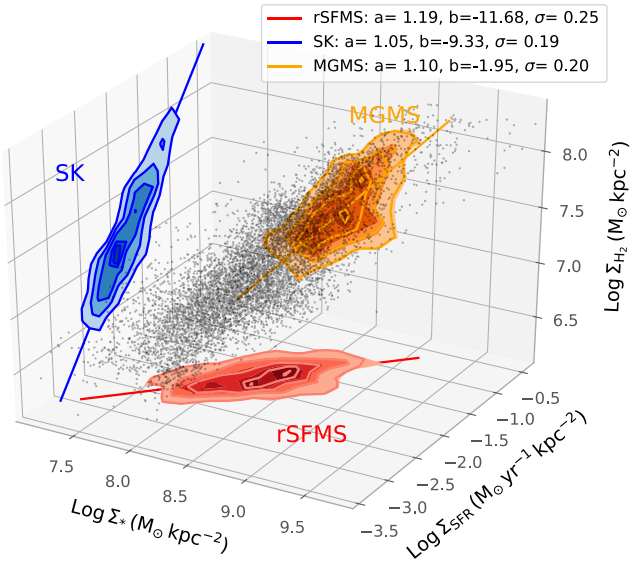

Figure 1. The 3D distribution between Σ_*, Σ_{H_2}, and Σ_{SFR}, computed for 5383 spaxels (black points) identified as star-forming regions taken from 14 ALMaQUEST (Lin et al. 2020) main sequence galaxies. The contours show the results projected on the 2D planes (red: rSFMS; blue: rSK; orange: rMGMS), with the contour levels corresponding to 20%, 40%, 60%, 80%, and 90% of the density peaks. The best-fit parameters and associated scatters (σ) based on ODR fitting are given in the legend. Figure taken from Lin et al. (2019).

Fig. 2 plot shows the resolved SFMS relation, left for the star-forming spaxels and right for the retired spaxels. The top panels are for the MS galaxies while the bottom panels are for the GV galaxies. The blue dotted line represents the original SFMS and is shown in every panel to guide our eyes. As expected (or by definition), the retired spaxels lie below the MS line. However, what is interesting here is that the relations between MS and GV are different even if we only focus on the star-forming spaxels of MS galaxies. Bearing in mind that the ratio of SFR to M_* is sSFR, this means that the sSFR of star-forming spaxels of GV galaxies is lower compared to that of MS galaxies Lin et al. (2022).

Next, we show the resolved SK relation in Fig. 3. As we reported in Lin et al. (2022), the retired spaxels lie well below the reference line, meaning that the star formation efficiency (SFE), defined as SFR divided by M_{H_2}, is pretty low in these retired regions as opposed to the star-forming spaxels. And how about the star-forming spaxels between MS and GV galaxies? If we compare the solid line, which is the best-fit for the GV galaxies, to the reference line from MS galaxies, you can see that the GV deviates from the MS galaxies toward a lower value of SFE.

Similarly, we can compare the resolved MGMS between MS and GV galaxies, as well as between the star-forming and retired spaxels as discussed in Lin et al. (2022). Fig. 4 shows that the retired spaxels also lie well below this reference line, in other words, a lower gas fraction (f_{H2}) compared to the star-forming spaxels. When comparing the star-forming spaxels between GV and MS galaxies, although the difference is small, the normalization of GV galaxies is still found to be 3-σ lower compared to that of the MS galaxies.

From the above analyses, we found that statistically GV galaxies show lower f_{H2} and lower SFE compared to the MS galaxies. On the other hand, we know that from the work by Ellison et al. (2021), each of the resolved scaling relations actually shows a lot of

https://doi.org/10.1017/S1743921322004410 Published online by Cambridge University Press

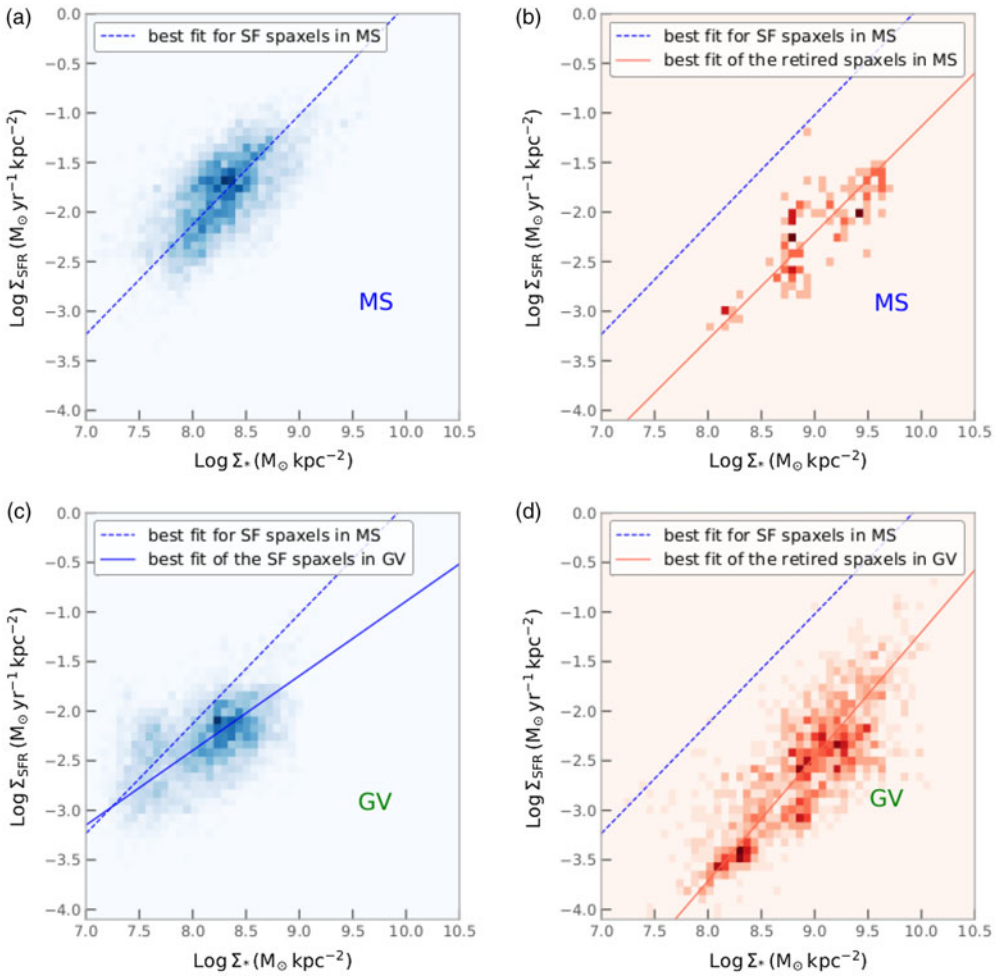

Figure 2. Number densities of star-forming (left panels; blue scales) and retired (right panels; red scales) spaxels on the rSFMS plane for MS (top panels) and GV (bottom panels) galaxies. The solid lines represent the best fit of the data points (blue for star-forming spaxels and red for retired spaxels) shown in each panel. The blue dashed lines are the same reference lines in each panel, corresponding to the best fit of the rSFMS derived for the star-froming spaxels in MS galaxies (i.e. a fit to the spaxels in the top left panel). Figure from (Lin et al. 2022).

galaxy-to-galaxy variation. So the next question we can ask is whether the deficit of gas and the inefficiency of star formation coexist in every single GV galaxy, or some galaxies show lower gas fractions whereas some others have lower SFE.

To investigate this issue, for each GV, we plot the spaxels with suppressed sSFR on the ΔSFE vs. Δf_{H2} plane (Fig. 6). An one-to-one line is plotted in each panel. If most spaxles lie above this line, it means that the low sSFR of this galaxy is under fuel-driven quenching. In contrast, if most spaxels lie below this line, it means that it is under efficiency-driven quenching. For the 15 GV galaxies that we are able to perform this classification, we found that roughly 40% are efficiency-driven, 33% are fuel-driven, and 27% have contributions from both factors. All these different situations are comparable, and there seems no dominant factor between fuel and efficiency driven that leads to the quenching in GV galaxies. Our results suggest that the mechanisms that cause the deficit of SFR in GV galaxies are likely case by case.

https://doi.org/10.1017/S1743921322004410 Published online by Cambridge University Press

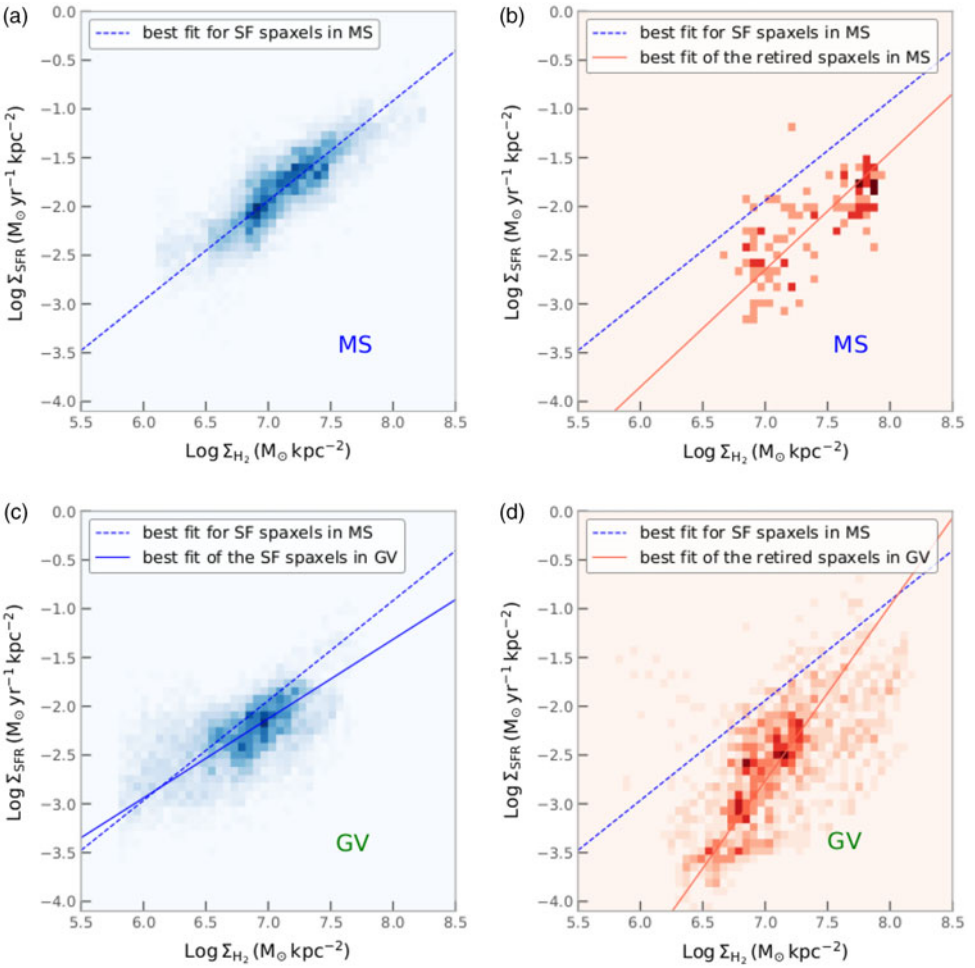

Figure 3. Similar to Fig. 2, but for the star formation rate surface density ($\Sigma_{\rm SFR}$) versus the molecular gas mass surface density ($\Sigma_{\rm H_2}$). Figure from Lin et al. (2022).

4. Dense gas

So far, our discussion was based on CO-based measurements. However, we know that it is the dense gas that is more directly relevant to star formation. The molecular gas-based SFE can be expressed as the dense gas SFE times the dense gas fraction (defined as the dense-to-molecular gas ratio), so the low CO-based SFE could be either due to the low dense gas star formation efficiency or the low dense gas fraction.

In order to distinguish these two effects, we follow up 5 ALMaQUEST galaxies with dense gas tracers, HCN and HCO^+ using ALMA. In Fig. 6, we show the CO-based SFE, versus the dense gas fraction. The blue dots are star-forming spaxels, and the red colors denote spaxels classified as retired regions. The grey symbols are unclassified spaxels. We can see that the CO-based star formation efficiency is considerably lower in retired and unclassified regions compared to that in star-forming spaxels as we discussed previously, but their dense fraction is actually comparable to those of star-forming regions. There is no obvious correlation between the CO-based SFE and the dense gas fraction. If this is true, then we expect that the dense gas-based SFE should be low for non-star forming regions.

https://doi.org/10.1017/S1743921322004410 Published online by Cambridge University Press

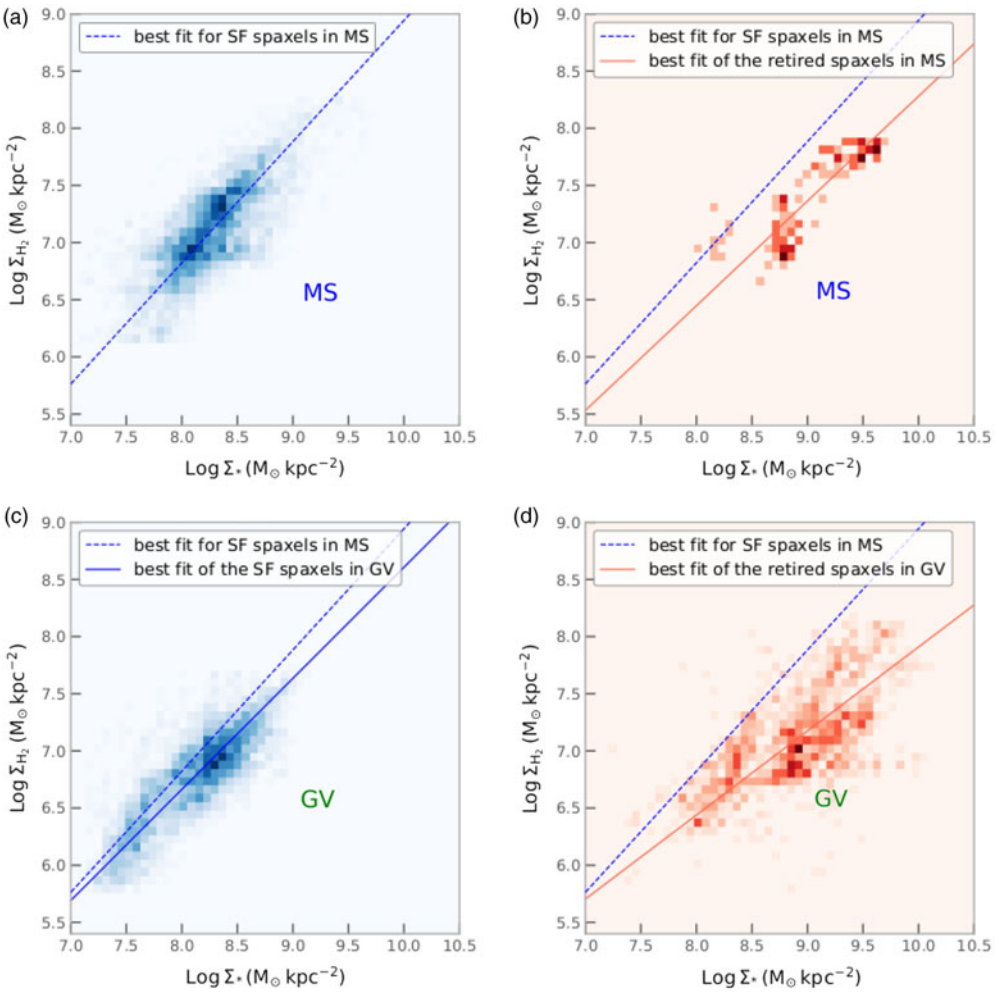

Figure 4. Similar to Fig. 2, but for molecular gas mass surface density (Σ_{H_2}) versus the stellar mass surface density (M_*) relation. Figure from Lin et al. (2022).

This is exactly what we see in the dense gas Schmidt-Kennicutt relation as shown in Fig. 7. We can see that while the star-forming spaxels form a clear correlation between the SFR and the dense gas surface density, the non-star-forming regions lie below the resolved SK relation formed by the star-forming spaxels and hence show lower dense gas SFE. In other words, there is some process that prevents even the dense gas from forming stars, leading to the overall low SFE (defined by the CO-based measurement), despite that they still have the dense gas.

5. Summary

The advent of spatially resolved stellar and gas observations has unveiled crucial links between the star formation rate, stellar mass, and molecular gas mass at (sub)kpc scales. These local relationships provide new insight to the understanding of global relationships. The major issues touched in this talk can be summarized as below:

https://doi.org/10.1017/S1743921322004410 Published online by Cambridge University Press

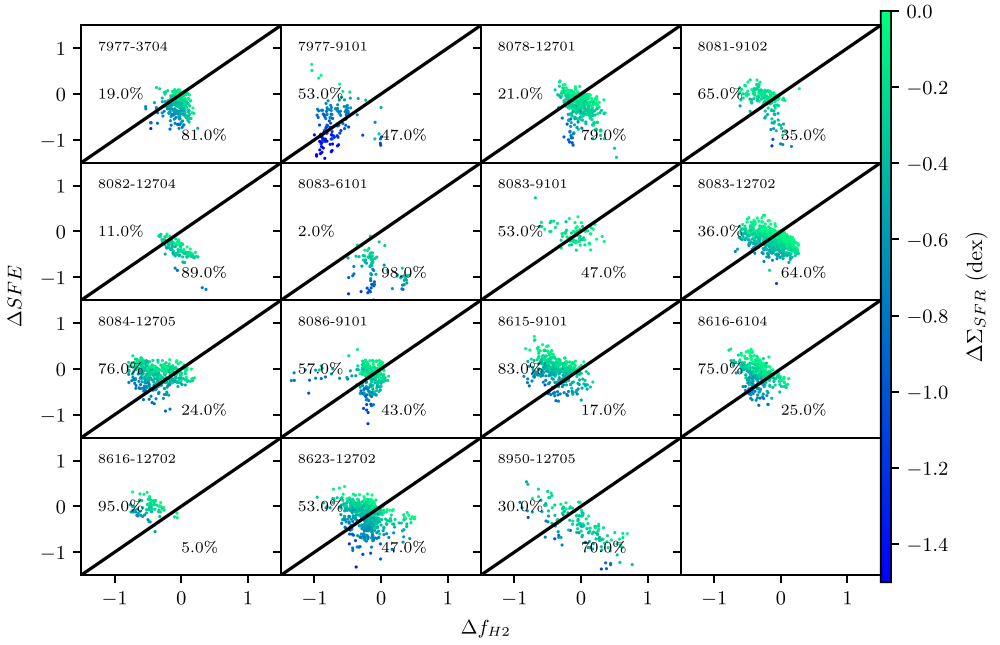

Figure 5. The spaxel-by-spaxel based ΔSFE versus Δf_{H2} in our GV sample, color coded by the ΔSFR. The fractions of spaxels locating on either side of the one-to-one solid line separating the SFE-driven and f_{H2} driven contributions are shown in each panel. Figure from Lin et al. (in prep.).

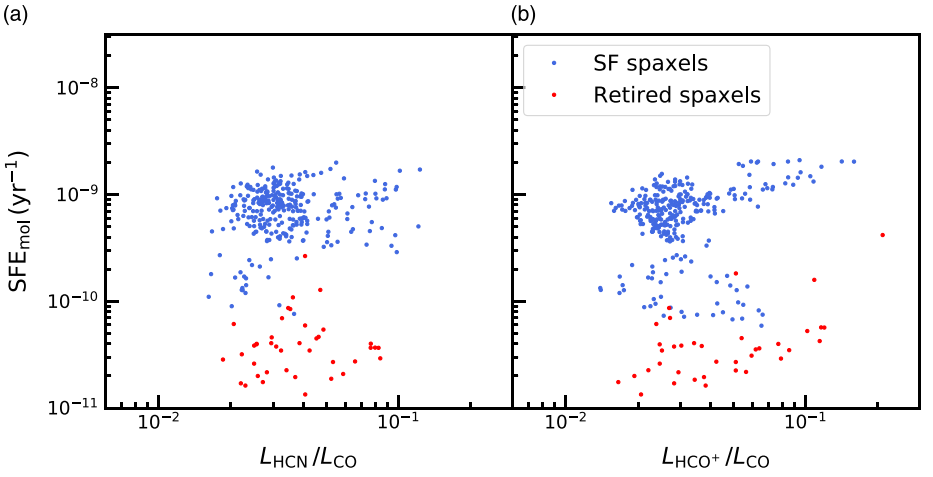

Figure 6. The CO-based star formation efficiency as a function of HCN-to-CO luminosity ratio (left panel) and HCO^+-to-CO luminosity ratio. The blue dots are star-forming spaxels, and the red colors denote spaxels classified as retired regions. The grey symbols are unclassified spaxels. Figure from Lin et al. (in prep.).

• Spatially resolved observations offer promising opportunities to probe the scaling relations of galaxies at kpc scales. Each pair of the 3 parameters, SFR, M_*, and M_{H_2} surface densities form a tight relation, referred to as rSFMS, rSK, and rMGMS, respectively. The rSFMS is suggested to be a by-product of the other two relations.

https://doi.org/10.1017/S1743921322004410 Published online by Cambridge University Press

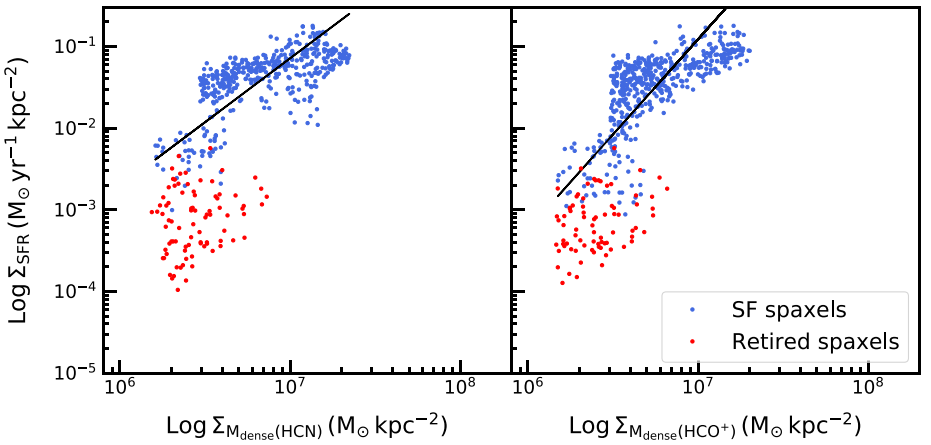

Figure 7. The dense gas version of the resolved Schmidt-Kennicutt relation in our sample. Left: HCN is used as the dense gas tracer. Right: HCO^+ is used as the dense gas tracer. The blue dots are star-forming spaxels, and the red colors denote spaxels classified as retired regions. The grey symbols are unclassified spaxels. Figure from Lin et al. (in prep.).

• The green valley galaxies show distinct scaling relations from the main sequence galaxies, having lower star formation efficiency and lower molecular gas fraction, even in the star-forming spaxels.

• The low CO-based star formation efficiency (SFE) of green valley galaxies is more associated with the low dense gas SFE, rather than the lower dense-to-molecular gas ratio.

Acknowledgements

LL thanks the conference organizers for their invitation. We also thank the ALMaQUEST members and other co-authors on the work described in this talk. A significant amount of the work presented here is based on the MaNGA survey and the precious ALMA observations.

References

Bolatto, A. D., Wong, T., Utomo, D., et al. 2017, ApJ, 846, 159
Brownson, S., Belfiore, F., Maiolino, R., et al. 2020, MNRAS, 498, L66
Daddi, E., Dickinson, M., Morrison, G., et al. 2007, ApJ, 670, 156
Ellison, S. L., Lin, L., Thorp, M. D., et al. 2021, MNRAS, 501, 4777
Kennicutt, R. C., Jr. 1998, ApJ, 498, 541
Leroy, A. K., Schinnerer, E., Hughes, A., et al. 2021, ApJS, 257, 43
Lin, L., Dickinson, M., Jian, H.-Y., et al. 2012, ApJ, 756, 71
Lin, L., Belfiore, F., Pan, H.-A., et al. 2017, ApJ, 851, 18
Lin, L., Pan, H.-A., Ellison, S. L., et al. 2019, ApJL, 884, L33
Lin, L., Ellison, S. L., Pan, H.-A., et al. 2020, ApJ, 903, 145
Lin, L., Ellison, S. L., Pan, H.-A., et al. 2022, ApJ, 926, 175
Morselli, L., Rodighiero, G., Enia, A., et al. 2020, MNRAS, 496, 4606
Noeske, K. G., Faber, S. M., Weiner, B. J., et al. 2007, ApJ, 660, L47
Pessa, I., Schinnerer, E., Belfiore, F., et al. 2021, A&A, 650, A134
Sánchez, S. F., Barrera-Ballesteros, J. K., Colombo, D., et al. 2021, MNRAS, 503, 1615
Schmidt, M. 1959, ApJ, 129, 243
Sorai, K., Kuno, N., Muraoka, K., et al. 2019, PASJ, 71, S14.
Speagle, J. S., Steinhardt, C. L., Capak, P. L., & Silverman, J. D. 2014, ApJS, 214, 15
Whitaker, K. E., van Dokkum, P. G., Brammer, G., et al. 2012, ApJ, 754, L29

https://doi.org/10.1017/S1743921322004410 Published online by Cambridge University Press